ELSEVIER

Thermochimica Acta 273 (1996) 239–255

thermochimica acta

A kinetic and mechanistic study of the isothermal decomposition of calcium maleate dihydrate and calcium fumarate trihydrate

Andrew K. Galwey [a], Mohamed Abdel-Aziz Mohamed [b]

[a] *School of Chemistry, Queen's University of Belfast, Belfast BT9 5AG, Northern Ireland, UK*
[b] *Department of Chemistry, Faculty of Science, South Valley University, Qena 83511, Egypt*

Received 20 March 1995; accepted 16 June 1995

Abstract

The kinetics of the isothermal decomposition of calcium maleate dihydrate (between 460 and 490°C) and calcium fumarate trihydrate (between 460 and 530°C) were studied. Kinetic measurements were carried out using the accumulatory method for the evolution of permanent product gases in a calibrated pre-evacuated glass apparatus. The product gases, from both reactants, were shown by mass spectrometry to be dominated by CO_2 with relatively smaller amounts of CO, C_2H_2 and C_2H_4. The solid decomposition products, from both reactants, were identified using X-ray powder diffraction and IR spectroscopy as a mixture of $CaCO_3$ and $Ca(OH)_2$ together with carbonaceous residue.

Due to the uncertainity of the composition of the solid residue, approximate reaction stoichiometry for the decomposition of both reactants is given.

Analysis of kinetic data was somewhat complicated by the intervention of a secondary reaction possibly involving gaseous species. Kinetic data of both reactants were found to fit the zero-order equation in the range $0.05 < \alpha < 0.47$. Afterwards, data were best fitted to the second-order rate equation in the range $0.47 < \alpha < 0.78$.

NMR analysis of partially decomposed calcium maleate showed no isomerization to the more stable fumarate anion.

Scanning electron microscopy (SEM) revealed that neither of these two reactants underwent comprehensive melting during the decomposition reaction.

Keywords: Carboxylate; Isothermal; Kinetics; Pyrolysis

SSDI 0040-6031(95)02582-0

1. Introduction

Kinetic and mechanistic studies of the thermal decompositions of a wide variety of metal carboxylates have revealed relatively few patterns and trends of similarities of behaviour [1]. Exceptions to this generalization include the observation that the breakdown of a number of metal malonates proceed with the intervention of the corresponding metal acetate which later decomposes. This behaviour has been described for the thermal reactions of copper [2], calcium [3], nickel [4] and manganese [5] malonates. The decomposition of some metal acetates has been shown to proceed with the intermediate production of basic metal salts, for example lead [6] and nickel [7] acetates. In contrast, other metal acetates, including those of cobalt [8] and manganese [9], proceed through the intervention of acetyl metal acetates. It has also been shown that the decompositions of the following copper(II) carboxylates proceed through two rate processes with stepwise cation reduction ($Cu^{2+} \rightarrow Cu^{+} \rightarrow Cu^{0}$): oxalate [10], malonate [2], maleate and fumarate [11], squarate [12] (though this is not a carboxylate) and, more recently, mellitate [13].

The thermal reactions of metal carboxylates appear, therefore, as a field within which many studies have been completed [1] but in which there has been less progress in recognizing the factors that control reactivity and chemical behaviour. We have, therefore, undertaken the present investigations of the decompositions of calcium maleate and of calcium fumarate to compare behaviour of these reactants containing the divalent (only) strongly electropositive cation with previous observations for transition metal (copper and nickel) salts containing the same anions. Organic acids containing unsaturated anions are to be preferred for comparative rate studies to reduce the number of possible hydrocarbon products and secondary reactions.

The decompositions in vacuum of copper(II) maleate and of copper(II) fumarate have been shown [11] to involve two reactions. The maleate first underwent isomerization to the more stable fumarate ion and there was cation reduction ($Cu^{2+} \rightarrow Cu^{+}$) with evidence of at least some melt formation. Decomposition of the fumarate also involved stepwise cation reduction but there was apparently no melting. Taki et al. [14] reported that copper maleate and copper fumarate evolved ethylene as the predominant product of the thermal reaction whereas acetylene was the dominant product from the laser-induced reaction. This difference was ascribed to the faster heating rate in the laser-promoted reaction.

Nickel maleate was reported to decompose in vacuum [15] to yield a nickel and carbon residue between 270 and 310°C, while nickel fumarate [16] decomposed at a slightly higher temperature, 300–340°C, to yield mainly nickel carbide, Ni_3C.

In a recent non-isothermal study of the decomposition of silver maleate dihydrate and anhydrous silver fumarate, Mohamed et al. [17] reported that both compounds showed some sublimation prior to decomposition. Silver maleate was found to isomerize on heating above 230°C to the more stable fumarate anion. Gaseous decomposition products were dominated by maleic anhydride and CO_2 with minor proportions of ethylene, ethyl alcohol, acetone, methane and isobutene. Silver metal was identified as the final solid product from reactions of both compounds.

The main objective of the present study is to compare the behaviour of the present two reactants with the previous studies of copper(II), nickel and silver maleates and fumarates [11, 15–17]. We are aware of no previous study concerned with the thermal decompositions of calcium maleate or calcium fumarate.

2. Experimental

2.1. Preparation of reactant salts

2.1.1. Calcium maleate dihydrate

This salt was prepared by the slow addition, with continuous stirring, of 10 g of $CaCO_3$ (AnalaR) to an aqueous solution containing a slight stoichiometric excess of maleic acid (approx. 11.7 g) in 300 ml of distilled water maintained at 80°C. After complete addition of the $CaCO_3$, the solution containing a white precipitate was kept at 80°C for 3 h followed by 12 h at ambient temperature before filtration. The precipitate was washed several times with distilled water and finally dried in air.

2.1.2. Calcium fumarate trihydrate

This salt was prepared by the addition of the stoichiometric amount of $CaCO_3$ to a solution containing a slight excess of fumaric acid in ethyl alcohol. The precipitate was separated by the same procedure as that described for the preparation of calcium maleate.

All chemicals used in the preparation of both reactant salts, i.e. fumaric acid, maleic acid and calcium carbonate, were analytical grade materials of high purity and, therefore, were used without further purification.

2.2. Kinetic measurements

Isothermal (± 1°C) kinetic measurements were performed using a constant volume pre-evacuated (for 2 h at 10^{-5} Torr) glass apparatus, a description of which is given elsewhere [12]. The pressure of the evolved volatile gaseous products of anion disintegration (CO_2, CO, C_2H_2 and C_2H_4) was measured using an MKS 222B Baratron absolute pressure gauge. A refrigerant trap (either solid/liquid methanol at −98°C or liquid nitrogen (−196°C)) was maintained between the heated reactant and the pressure gauge to condense water and other possible non-volatile products. Data, including measured time, temperature and pressure values, were recorded automatically, as previously described [2].

2.3. NMR spectroscopy

NMR spectroscopy was used to monitor, and measure quantitatively, the organic anions present, thereby identifying all isomeric transformations that take place during the decomposition process. Reactant samples that had been decomposed to various known extents (α, fractional reaction) were dissolved in D_2O and DSS was used as

a marker. All identifications were confirmed by adding the anion recognized and demonstrating an enhanced response for the specific peak, without the appearence of others. Confirmations also included the use of alternative solvents and ^{13}C NMR.

2.4. Scanning electron microscopy (SEM)

Samples of reactants together with samples of salt partially decomposed to various known α (fractional reaction) values as well as the products of complete decomposition ($\alpha = 1.0$) were examined in a JEOL 35 CF scanning electron microscope. Some samples were slightly crushed prior to investigation to reveal the structures of the intracrystalline materials [18].

3. Results and discussion

3.1. Elemental analysis

Both reactants were subjected to combustion analysis to determine the carbon and hydrogen contents. Calcium was determined by atomic absorption spectroscopy. The results of these analyses are given in Table 1 and satisfactorily confirm the identities of both reactants.

3.2. Reaction stoichiometry

The stoichiometry of the decomposition of calcium maleate dihydrate betweeen 460 and 490°C, and of the decomposition of calcium fumarate trihydrate between 460 and 530°C, were found to be difficult to measure quantitatively. This is due to the uncertainity of the composition of the solid residues produced from both salts. Nevertheless, the reactions of these two salts could be approximately represented as follows:

For calcium maleate dihydrate

$$C_4H_2O_4Ca\cdot 2H_2O \rightarrow 1.0(CaCO_3 + Ca(OH)_2) + 2H_2O + 0.45CO_2 + 0.15(CO + C_2H_2 + C_2H_4) + [C_{2.8}O_{0.5}H_{0.6}]$$

Table 1
Elemental analysis of the prepared reactants

Salt	% Carbon	% Hydrogen	% Calcium
Calcium maleate (measured)	25.21	3.11	21.50
Theoretical dihydrate	25.26	3.18	21.38
Calcium fumarate (measured)	23.10	3.88	19.19
Theoretical trihydrate	23.10	3.87	19.25

For calcium fumarate trihydrate

$$C_4H_2O_4Ca\cdot 3H_2O \rightarrow 1.0(CaCO_3 + Ca(OH)_2) + 3H_2O + 0.7CO_2 + 0.3(CO + C_2H_2 + C_2H_4) + [C_{2.4}O_{0.1}H_{0.6}]$$

From the weight loss measurements ($37.5 \pm 1.5\%$ for calcium maleate dihydrate and $43 \pm 2\%$ for calcium fumarate trihydrate), it is concluded that the residual product contained approximately equimolar proportions of $CaCO_3$ and CaO. The latter reacted readily with water vapour to yield $Ca(OH)_2$ on exposure to the atmosphere. The presence of significant amounts of both $CaCO_3$ and $Ca(OH)_2$ in the residues was confirmed by infrared and X-ray diffraction measurements for the final residual products. $Ca(OH)_2$ is known [19] to decompose at temperatures (360–430°C) below those of the present reactions.

Water of crystallization was determined quantitatively from the weight loss that accompanied the dehydration under vacuum at 250°C for 60 min. The yield of permanent product gases, i.e. CO_2, CO, C_2H_2 and C_2H_4, was calculated from the final pressure measured following completed decompositions of known weights of reactant salt in the calibrated pre-evacuated glass apparatus as 0.60 mole of gas/mole of salt decomposed for calcium maleate and 1.0 mole/mole of salt decomposed for calcium fumarate.

The proportion of $CO + C_2H_2 + C_2H_4$ to CO_2 (approx. 25% for the maleate salt and 30% for the fumarate reactant) was calculated from the pressure registered in the presence of a liquid nitrogen trap (−196°C) compared to that pressure registered when methanol refrigerant (−98°C) was interposed. The amount of gases and the ratio of $CO + C_2H_2 + C_2H_4/CO_2$ for both reactant salts were taken from the average results of more than 30 experiments within the temperature ranges of the kinetic studies.

Mass spectrometry confirmed that CO_2 was the major gaseous product from both salts with the m/e value of 44. CO and C_2H_4 were shown, by mass spectrometry, to be present in smaller amounts with the m/e value of 28. Acetylene (C_2H_2) is also identified by its m/e value of 26. Ethylene and acetylene are identified as product gases because the oxygen content in both reactants is not sufficient to produce the observed pressure as CO_2 and CO only.

Finally, elemental carbon in the residue was determined in the solid products from both salts, by combustion analysis. These results showed the presence of 32% carbon in the maleate residual solid and 24% in the calcium fumarate residual solid.

3.3. Reaction kinetics

3.3.1. Calcium maleate dihydrate

Fig. 1 shows five representative isothermal α–time curves for the decomposition of calcium maleate dihydrate between 460 and 490°C using methanol refrigerant (−98°C). These curves showed that, after a short initial process, the reaction in the range $0.01 < \alpha < 0.9$ is deceleratory throughout. The fractional reaction (α) values were measured, here, from the total yield of gases, i.e. including CO_2, CO, C_2H_2 and C_2H_4.

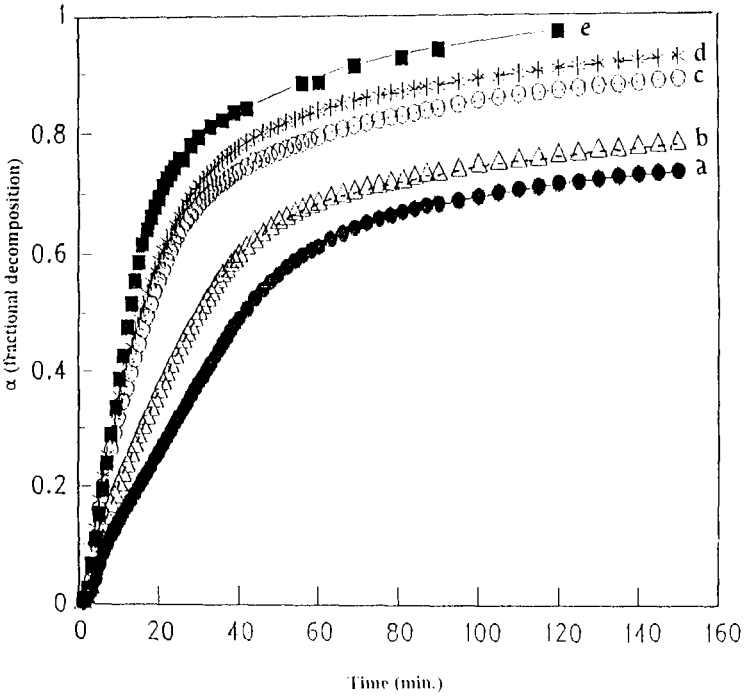

Fig. 1. Five representative isothermal α–time curves for the decomposition of calcium maleate dihydrate at the following temperatures: a, 470°C; b, 475°C; c, 480°C; d, 485°C, and e, 490°C.

Duplicate experiments were carried out at the same temperature where methanol refrigerant was used in one experiment and a liquid nitrogen trap was used in the other. The pressure of CO_2 present was calculated for each time from the difference in pressure reading for the methanol refrigerant experiment and the pressure reading in the presence of the liquid nitrogen trap. From these data, α-values were then calculated for CO_2 evolution only. Fig. 2 shows the α–time curves for an example of these duplicate experiments together with α–time curve calculated for the evolution of CO_2 alone.

Kinetic data of the decomposition of calcium maleate was found to fit the zero-order rate equation in the range $0.07 < \alpha < 0.48$. Fig. 3 shows the fitting of the data, presented in Fig. 1, of the first half reaction to the zero-order rate equation. The activation energy (ΔE) was calculated to be 81 ± 4 kcal mol^{-1} between 470 and 490°C in the presence of methanol refrigerant, i.e. for the evolution of all gases.

Above $\alpha = 0.5$, however, the kinetic data fitted the second-order rate equation, $kt = (1-\alpha)^{-1}$ [1]. Fig. 4 shows this fit for the same experiments as those shown in Fig. 1. The activation energy (ΔE) measured for the second half reaction was calculated as 104 ± 7 kcal mol^{-1}, i.e. about 1.3 times greater than the ΔE value measured for the first half reaction.

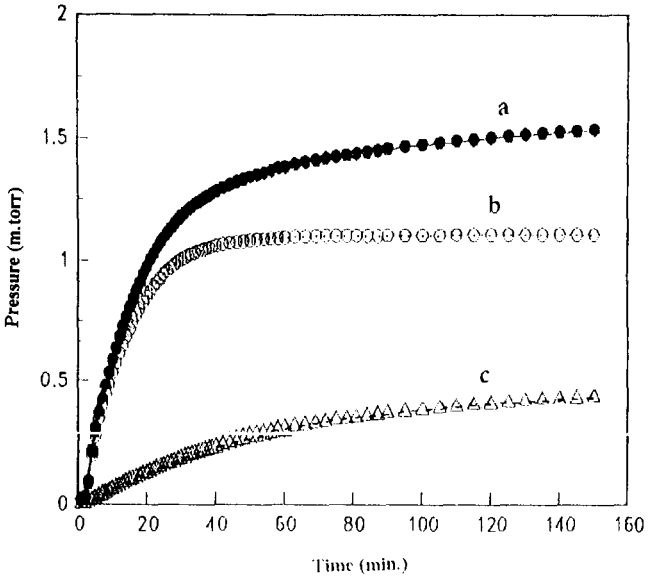

Fig. 2. Three pressure–time curves for the decomposition of calcium maleate dihydrate at 485°C showing: a, total gases; b, CO_2 only; and c, CO, C_2H_2 and C_2H_4.

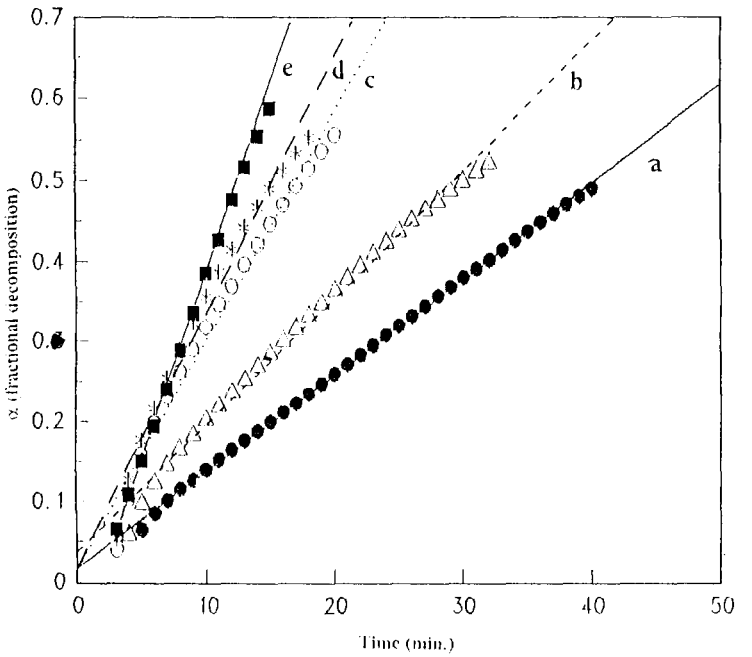

Fig. 3. The fit of kinetic data for calcium maleate dihydrate decomposition in the range $0.05 < \alpha < 0.48$ to the zero-order rate equation for the same experiments as shown in Fig. 1.

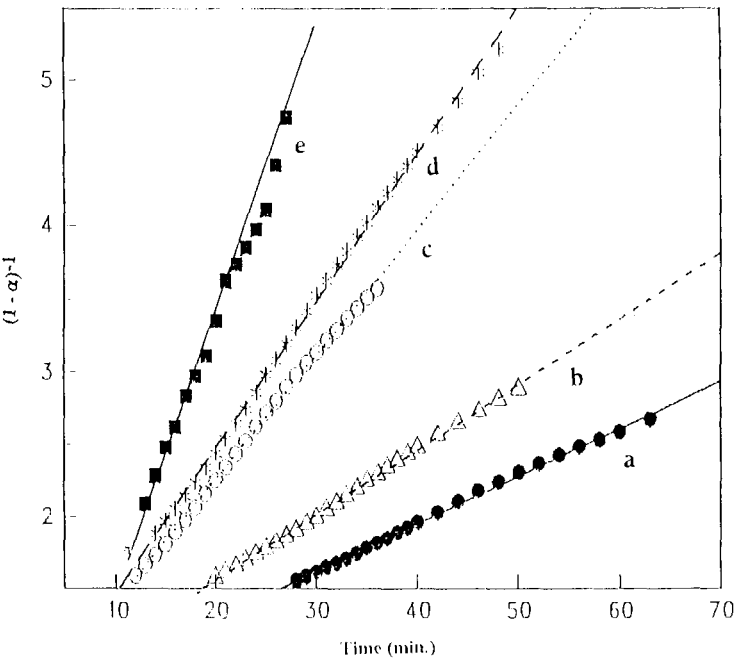

Fig. 4. Second-order plots of data for the decomposition of calcium maleate dihydrate at the following temperatures: a, 470°C; b, 475°C; c, 480°C; d, 485°C; and e, 490°C.

3.3.2. *Calcium fumarate trihydrate*

Representative isothermal α–time plots of the decomposition of calcium fumarate trihydrate are shown in Fig. 5. These curves are broadly similar to those of the maleate reactant. After an initial short reaction in the range $0.01 < \alpha < 0.09$, the data were again well represented by the zero-order rate equation in the range $0.05 < \alpha < 0.45$. The fit of the data of Fig. 5 to the zero-order rate equation is presented in Fig. 6. The activation energy (ΔE) for this part of the reaction was calculated to be 40 ± 2 kcal mol^{-1} (between 460 and 530°C). In the presence of methanol refrigerant, i.e. for the total gaseous products; the corresponding activation energy was found to be somewhat higher (approx. 44 ± 3 kcal mol^{-1}). The activation energy for the evolution of CO_2 only was calculated (from the pressure difference between methanol refrigerant and the pressure in the presence of liquid nitrogen at the same time and temperature) as 47 ± 4 kcal mol^{-1} (across the same temperature interval).

Following the zero-order behaviour, the data fitted well the second-order rate equation in the range $0.44 < \alpha < 0.75$. Fig. 7 shows the very satisfactory linear fit for the same group of experiments as shown in Fig. 5. The activation energy (ΔE) for the second half of the reaction (in the presence of methanol refrigerant) was calculated as 52 ± 4 kcal mol^{-1}. It is clear that the activation energy of the decomposition of calcium fumarate is much smaller than the corresponding values for the calcium maleate reactant.

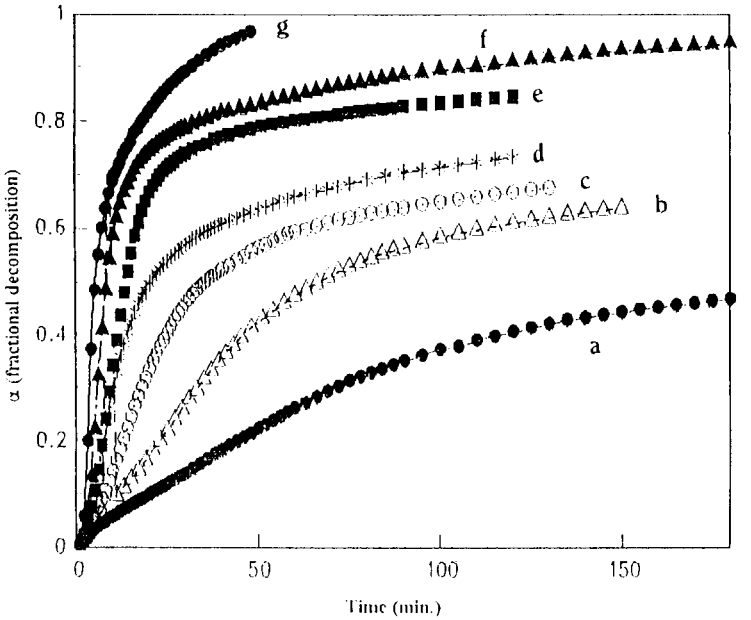

Fig. 5. Representative α–time curves for the decomposition of calcium fumarate trihydrate at the following temperatures: a, 460 °C; b, 470 °C; c, 480 °C; d, 490 °C; e, 500 °C; f, 515 °C; and g, 530 °C.

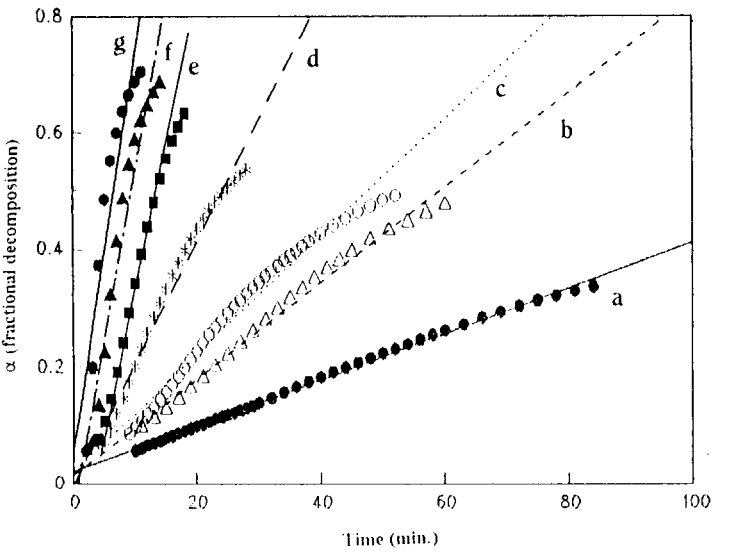

Fig. 6. The fit of kinetic data for calcium fumarate trihydrate decomposition in the range $0.07 < \alpha < 0.48$ to the zero-order rate equation for the same group of experiments as shown in Fig. 5.

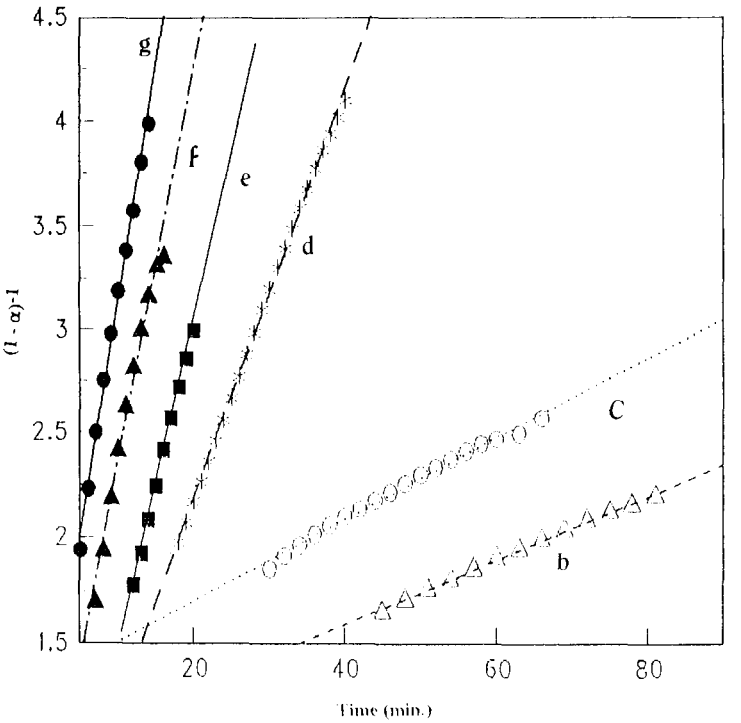

Fig. 7. Plots of the second-order fit for the data shown in Fig. 5 for the decomposition of calcium fumarate trihydrate between 470 and 530°C.

Similar duplicate experiments to those performed for the calcium maleate were carried out for calcium fumarate reactant. Fig. 8 shows three α–time curves representing decomposition at the same temperature. α-Values were calculated (for CO + acetylene + ethylene) using a liquid nitrogen trap, for the total yield of gases (using methanol refrigerant) and for CO_2 (from the pressure difference between measurements using methanol and liquid nitrogen traps).

The acceleratory nature of the α–time curves representing the evolution of CO_2 gas (Fig. 8) is evidence of an increase in the yield of product CO_2 gas at the expense of CO which could arise through the disproportionation reaction [20]

$$2CO \rightarrow CO_2 + C$$

3.4. *Effect of dehydration, crushing and weight of sample on reaction kinetics*

The effect of different variables on the kinetics of the decomposition of calcium fumarate trihydrate was studied. For this purpose a number of experiments were carried out at the same temperature (490 ± 1°C) with different sample pre-treatments. We can summarize the results of these experiments as follows:

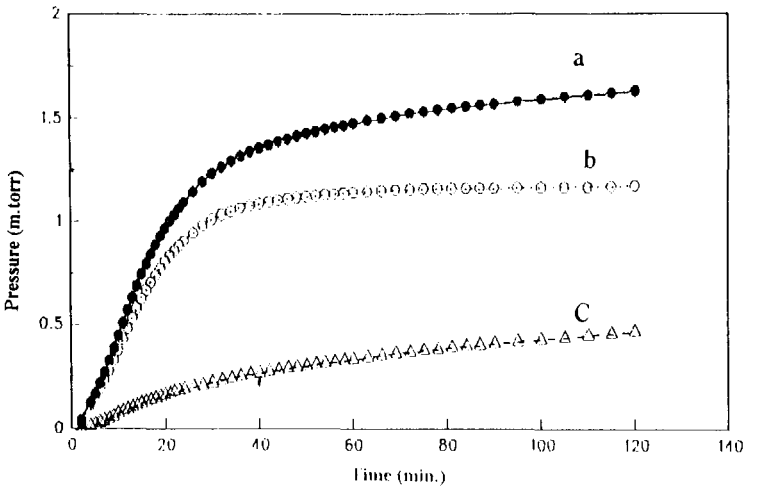

Fig. 8. Three pressure–time curves for the decomposition of calcium fumarate trihydrate at 490°C showing: a, total gases; b, CO_2 only; and c, CO, C_2H_2 and C_2H_4.

(1) Gentle crushing of the original reactant crystallites resulted in a reduction in the reaction rate (× 0.80).

(2) Doubling the weight of sample appreciably lowered the decomposition rate, particularly during the second half reaction (× 0.75).

(3) Dehydration of the reactant hydrate (at 200°C for 60 min) prior to the decomposition diminished the rate of decomposition more than that caused by all other factors, i.e. × 0.65.

3.5. *NMR analysis*

The original calcium maleate reactant gave a single response at 5.99–6.01 ppm, which corresponds to the maleate anion, in addition to the solvent (D_2O) response at 4.87 ppm. As the extent of decomposition (α) increases, the intensity of the maleate peak progressively decreases until it completely vanishes at $\alpha = 0.6$ without the appearance of further responses. This suggests that calcium maleate does not undergo any anion isomerization to the fumarate anion in contrast to copper maleate [11] and silver maleate [17] where this change was positively identified.

Calcium fumarate trihydrate reactant, however, gave a signal at 6.52 ppm due to the fumarate anion together with the solvent response at 4.87 ppm. Again, as the decomposition reaction proceeds, the intensity of the fumarate signal decreased and it vanished above $\alpha = 0.6$ with no other peaks having appeared.

It is worth noting here that IR spectroscopy was also used in order to investigate the possibility of anion isomerization. The results of the IR investigations showed, also, no evidence of any anion transformation during the course of decomposition of either reactant.

3.6. Scanning electron microscopy (SEM)

Investigations of sample textures for both reactants at different extents of decomposition (α) were carried out. Representative micrographs are shown in Fig. 9 for the calcium fumarate reactant. Micrographs 9(a, b) show the effect of dehydration on the large, approximately, rectangular-shaped crystallites (250 × 120 μm) for which the laminar structure appeared after the dehydration process. The flat, originally smooth, crystal faces became pitted and roughened. Micrograph 9(c) shows crystallites of a sample decomposed to $\alpha = 0.2$. The surfaces of these crystallites underwent extensive parallel cracking together with the appearance of some pores. Micrographs 9(d–f) are representative of other samples decomposed to $\alpha = 0.2$ and were subsequently gently crushed in order to expose their interior structures. The product here is characterized by its state of fine division and the coherent aggregation of these tiny particles. It shows also that the original outer boundary surfaces are still relatively smooth.

Micrographs 9(g, h) show samples decomposed to $\alpha = 0.8$. Extensive disintegration of the reactant crystallites is obvious and two different types of products are shown. Both structures are characterized by comparable particle sizes. A similar structure, to that seen in micrograph 9(g) was seen at an early stage ($\alpha = 0.2$) of the decomposition, see micrograph 9(f).

An exactly comparable series of electron microscopic textural examinations was completed for the decomposition of calcium maleate. Results were closely similar in all respects to those described for calcium fumarate and no new distinguishing features were found.

It is concluded from examination of the electron micrographs that neither of these salts underwent comprehensive melting during reaction. The textures of intracrystalline material were below our limits of microscopic resolution and the present observations do not permit the recognition of the participation of local and/or temporary melt

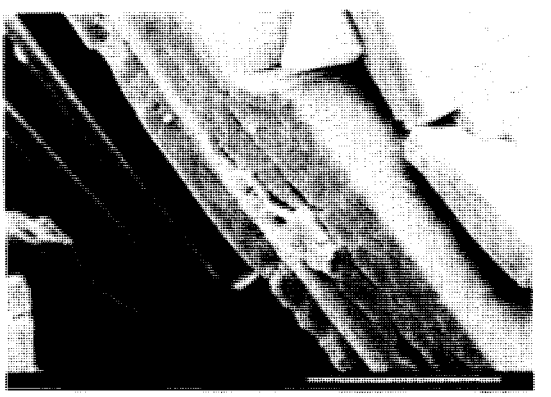

Fig. 9a. Representative scanning electron micrographs for the decomposition of calcium fumarate trihydrate at different measured α values: (a, b) dehydrated samples; (c) $\alpha = 0.2$, uncrushed; (d–f) $\alpha = 0.2$, crushed; (g, h) $\alpha = 0.8$, slightly crushed. Scale bars: a,b, 100 μm; c, 10 μm; d, 1μm; e, 10 μm; f, 1 μm; g,h, 1 μm.

Fig. 9b.

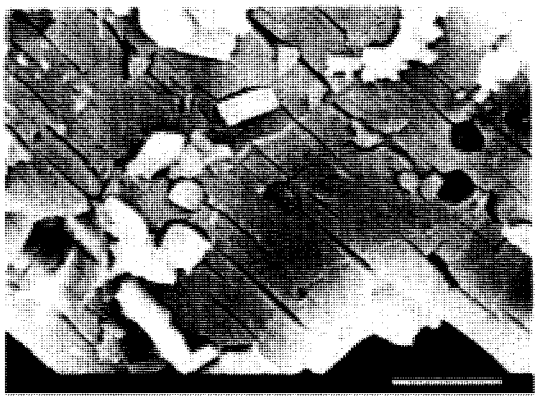

Fig. 9c.

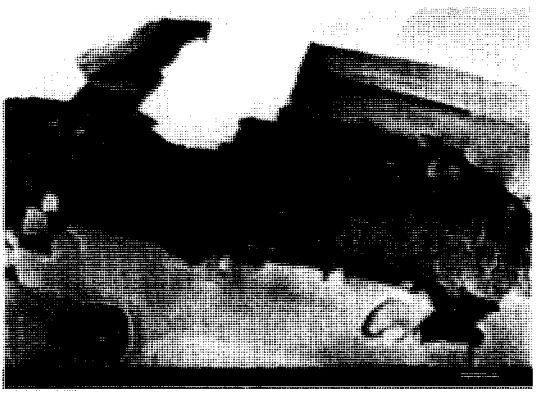

Fig. 9d.

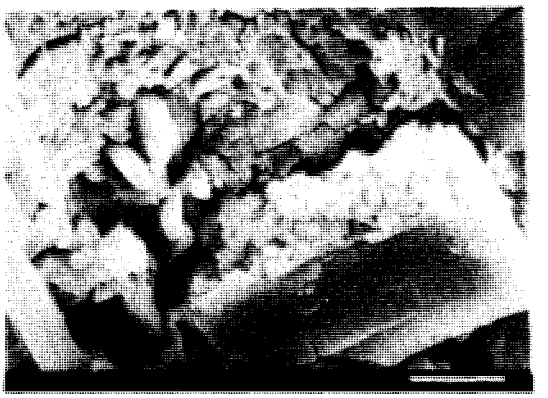

Fig. 9e.

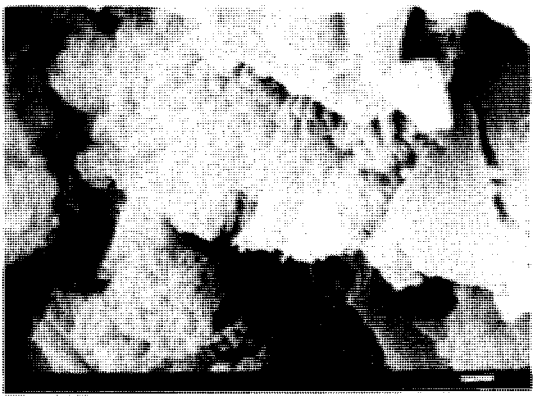

Fig. 9f.

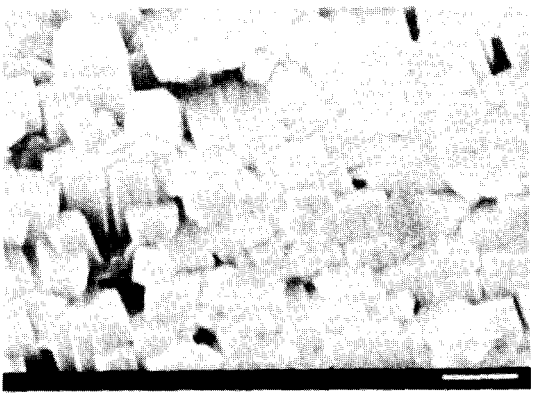

Fig. 9g.

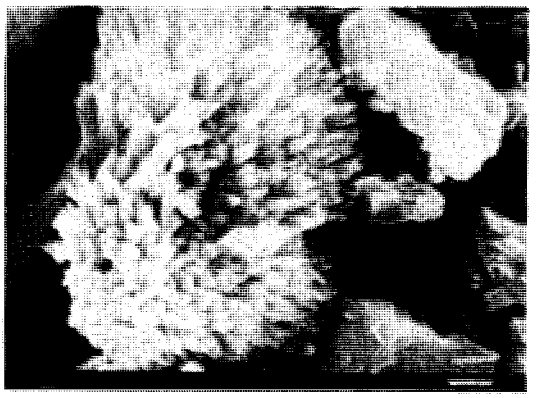

Fig. 9h.

formation. The internal textures were different from the crystal boundary surfaces where a superficial layer maintained particle individuality and perhaps prevented coalescence [2, 12]. The possible role of melting is therefore unresolved by the evidence available.

4. Discussion

4.1. Reaction products

The yields of carbon dioxide from decompositions of both reactants represent only approx. 50% of the constituent carboxyl groups and most of the remainder is retained in the residue as $CaCO_3 \cdot CaO$ (readily hydrated to $Ca(OH)_2$) is also formed in significant yield. Reduction of this electropositive metal is not expected under the present reaction conditions, in contrast with the behaviour observed for the copper(II) [11], nickel [15, 16] and silver [17] salts, all of which resulted in reduction of the cation to the metal (and Ni_3C in nickel salts).

We note from Figs. 2 and 8 that the gaseous products (CO, C_2H_2 and C_2H_4) continue to be evolved after the production of CO_2 is effectively completed at $\alpha = 0.7$–0.8. It is also observed from the NMR measurements that the reactants contain no detectable amounts of maleate or fumarate ions when $\alpha > 0.6$. We conclude, therefore, that (at least) two concurrent rate processes contribute to the overall reaction. The early stages of decomposition release involve carboxylate group breakdown to yield CO_2 which finally appears in approximately equal proportions as gas and as $CaCO_3$. A second unidentified non-volatile product must also be formed which undergoes relatively slower decomposition at reaction temperature. Because its breakdown evolves significant yields of C_2H_2 and C_2H_4, this must be a relatively stable polymeric material. It would appear, from the electron micrographs, that this is present intimately admixed with very fine solid reactant + $CaCO_3$ + CaO particles. The organic component is probably ill-crystallized and perhaps amorphous or semi-molten.

The absence of maleate isomerization to the more stable fumarate form at reaction temperature was unexpected [11,17]. This indicates a considerable stability of the reactant structure, probably arising from strong Ca^{2+} ion bonding to the carboxyl groups so that significant loosening, e.g. by melting, does not occur prior to anion breakdown.

4.2. Reactivity and reaction kinetics

The present reactions occur in a temperature interval (> approx. 460°C) that is significantly above the range of decompositions of most carboxylates [1]. This is ascribed to the electropositive character of the cation and the consequent strength of the calcium to oxygen link, identified as a controlling parameter in these reactions [21,22]. The decomposition of calcium malonate [3], studied in a significantly lower temperature range (340–380°C), was identified as proceeding through a mechanism in which control involved essential hydrogen transfer steps. The diminished availability and reactivity of hydrogen bonded to unsaturated carbon in the present reactants is consistent with this previous conclusion and the observed greater stability of the present salts.

Precise kinetic analyses of the present rate processes are not possible because it is not known whether the proportion of CO_2 evolved as gas and that retained as $CaCO_3$ remained constant during reaction. Furthermore, the electron microscopic observations gave no evidence as to whether reaction proceeded at an advancing reaction interface (reactant/product) [1]. We also note that carboxylate ion breakdown was accompanied by the relatively slower rate process yielding C_2H_2, C_2H_4 and CO which further complicates the kinetic analyses. The reaction rate of calcium fumarate was significantly diminished by pre-dehydration, pre-crushing or a rise in sample mass. These changes are attributable to effects resulting from secondary reactions, probably involving gaseous species, within the reactant crystallite aggregate. Evidence of the significant role of secondary reactions reduces the reliability of the mechanisms proposed and only a semi-quantitative analysis of kinetic data is possible here.

The shapes of the α–time curves for both reactions were closely similar (Figs. 1 and 5; Figs. 2 and 8). Zero-order behaviour was observed for the evolution of about half of the product gas followed by a strongly deceleratory process that was well represented by the second-order rate equation.

The initial constant rate can alternatively be regarded as the composite outcome of two (or more) different but unresolved decompositions: a nucleation and growth process overlapping with a deceleratory reaction, or interface advance inwards in flat crystallites. (In the latter model, crushing reduced the rate by the detachment of adherent product that initiates reaction.) No mechanistic significance can be attached to magnitudes of the calculated activation energies for overlapping concurrent processes.

The deceleratory second rate process, observed after the breakdown of all maleate or fumarate in the reactant, is ascribed to pyrolysis of the products of salt decomposition. The second-order fit is explained by progressive diminution in the amount present accompanied by progressive diminution in the ease of reaction as reactivity is lost through the removal of hydrogen as C_2H_2 and C_2H_4.

Acknowledgements

We thank the staff of the electron microscope unit (QUB) for help and advice in obtaining the electron micrographs.

References

[1] M.E. Brown, D. Dollimore and A.K. Galwey, Comprehensive Chemical Kinetics, Vol. 22, Reactions in the Solid State, Elsevier, Amsterdam, 1980.
[2] N.J. Carr and A.K. Galwey, Proc. R. Soc. London, Ser. A, 404 (1986) 101.
[3] A.K. Galwey and M.A. Mohamed, Solid State Ionics, 42 (1990) 135.
[4] A.K. Galwey, S.G. McKee, T.R.B. Mitchell, M.A. Mohamed, M.E. Brown and A.F. Bean, React. Solids, 6 (1988) 187.
[5] M.A. Mohamed, J. Anal. Appl. Pyrol., 30 (1994) 59.
[6] M.A. Mohamed, S.A. Halawy and M.M. Ebrahim, Thermochim. Acta, 236 (1994) 249.
[7] M.A. Mohamed, S.A. Halawy and M.M. Ebrahim, J. Anal. Appl. Pyrol., 27 (1993) 109.
[8] M.A. Mohamed, S.A. Halawy and M.M. Ebrahim, J. Therm. Anal., 41 (1994) 387.
[9] M.A. Mohamed and S.A. Halawy, Thermochim. Acta, 242 (1994) 173.
[10] M.A. Mohamed and A.K. Galwey, Thermochim. Acta, 217 (1993) 279.
[11] N.J. Carr and A.K. Galwey, J. Chem. Soc. Faraday Trans. 1, 84 (1988) 1357.
[12] A.K. Galwey, M.A. Mohamed, S. Rajam and M.E. Brown, J. Chem. Soc. Faraday Trans. 1, 84 (1988) 1349.
[13] A.K. Galwey and M.A. Mohamed, Thermochim. Acta, 239 (1994) 211.
[14] K. Taki, R.H. Kim and S. Namba, Bull. Chem. Soc. Jpn., 43 (1970) 1450.
[15] M.J. McGinn, B.R. Wheeler and A.K. Galwey, Trans. Faraday Soc., 67 (1971) 1480.
[16] M.J. McGinn, B.R. Wheeler and A.K. Galwey, Trans. Faraday Soc., 66 (1970) 1809.
[17] M.A. Mohamed, S.A.A. Mansour and G.A.M. Hussien, J. Therm. Anal., 41 (1994) 405.
[18] A.K. Galwey and M.A. Mohamed, Proc. R. Soc. London, Ser A, 396 (1984) 425.
[19] A.K. Galwey and G.M. Laverty, Thermochim. Acta, 228 (1993) 359.
[20] F.A. Cotton and G. Wilkinson, Advanced Inorganic Chemistry, A Comprehensive Text, 4th. edn., J. Wiley, New York, 1980.
[21] M.A. Mohamed and A.K. Galwey, Thermochim. Acta, 213 (1993) 269.
[22] R.J. Acheson and A.K. Galwey, J. Chem. Soc. A, (1967) 1167.